

# PROGRESSIVE DAMAGE IN STITCHED COMPOSITES UNDER IMPACT LOADING

K.T. Tan<sup>1\*</sup>, N. Watanabe<sup>1</sup>, A. Yoshimura<sup>2</sup>, Y. Iwahori<sup>2</sup>, T. Ishikawa<sup>2</sup>

<sup>1</sup> Department of Aerospace Engineering, Tokyo Metropolitan University, Tokyo, Japan,

<sup>2</sup> Advanced Composite Technology Centre, Japan Aerospace Exploration Agency, Tokyo, Japan

\* Corresponding author ([tan-kwektze@sd.tmu.ac.jp](mailto:tan-kwektze@sd.tmu.ac.jp))

**Keywords:** *stitching, impact, quasi-static indentation, damage progression, delamination*

## 1 Introduction

Damage in carbon fibre reinforced plastics (CFRP) due to impact loading is an extremely complex phenomenon that comprises of multiple failure mechanisms like intra-laminar matrix cracks, inter-laminar delamination, fibre pull-out and fibre fracture. In stitched composites, impact damage behavior is further complicated by the presence of through-thickness stitching [1, 2], which not only favorably increases mode I/II interlaminar strength [3, 4], but also inevitably creates geometrical defects like weak resin-rich pockets around stitch threads and misalignment of in-plane fibres. Computational modeling has been used to simulate progressive damage effectively [5]. However, the complexity of impact damage progression in stitched composites would need to be first understood and appreciated by physical experimental observations.

In this study, quasi-static indentation (QSI) test is performed for the first time on stitched composites. QSI offers a good validation and comparison with low-velocity impact (LVI) test [6], and provides good understanding on damage progression in composite structures under impact loading. Damage initiation, propagation and ultimate failure are investigated due to the effect of stitching, particularly the influence of stitch density. Non-destructive evaluation (NDE) techniques namely ultrasonic c-scan analysis, x-ray radiography and x-ray micro computed tomography are employed to elucidate various damage mechanisms in stitched composites.

## 2 Experimental Details

### 2.1 Test Specimens

The specimens were made using T800SC-24K (Toray Industries) carbon fibre fabric of 20-ply

[+45/90/-45/0/0/+45/90/90/-45/0]<sub>s</sub>. The linear density of Vectran stitch threads used in this study is 200denier, with a stitch space and pitch of 3mm x 3mm (densely stitched) or 6mm x 6mm (moderately stitched). Vectran is selected as the stitch fibre because, besides having comparable properties with Kevlar, it is more superior due to its very low propensity to absorb moisture and performs better in interlaminar strengthening of stitched composites [7]. The type of stitch used is the Modified Lock stitch. After the stitching process (if any), resin transfer moulding (RTM) technique, using resin XNR/H6813, was adopted to consolidate the composite. Specimens of 100mm width and 150mm length were then cut out from a mother plate using a diamond wheel cutter. The averaged plate thickness of the 20-ply specimen is 4.1mm. All specimens are physically examined for any poor-resin regions and ultrasonic C-scanned for any internal delamination to ensure that they are free from any manufacturing related defects.

### 2.2 Experimental Methodology

Quasi-static indentation (QSI) test was performed using Instron 8852 test machine (100kN load cell) with a displacement rate of 0.5mm/min. The semi-spherical indenter has a diameter of 15.9mm and the specimen was placed on a support frame similar to the one used in the low-velocity impact (LVI) test [1, 2]. After each indentation step of 0.5mm, the specimen was unloaded and observed for damages, by conducting ultrasonic inspections using a 5 MHz probe and X-ray inspections using ZnI<sub>2</sub> penetrant. The specimen was subjected to both x-ray radiography and x-ray micro-computed tomography examination to observe in-plane and cross-sectional damages respectively. More details on these non-destructive evaluation techniques can be referred to [8]. After damage inspection, the specimen was

again subjected to indentation at higher loading at the next 0.5mm step. By repeating these steps, damage progression of stitched composite was investigated. The test was terminated once final failure was reached. This test was similarly repeated for all unstitched and stitched composites.

### 3 Results and Discussion

#### 3.1 Load-Displacement Curves

Typical Load-Displacement curves obtained from the quasi-static indentation tests are presented in Fig. 1. It is observed that damage progression can be categorized into three stages: *damage initiation*, *damage propagation* and *final failure*.

*Damage initiation* is characterized by the first observable slope change in the load-displacement graph, which often occurs between 1.0mm to 1.5mm indentation displacement in this study. *Final failure* is identified by the maximum force in the load-displacement curve, which is accompanied by an abrupt load drop. Final failure occurs during the 7.5mm step for densely stitched composites (Fig. 1a), and the 8.5mm step for moderately and unstitched specimens (Fig. 1b, c). The force values of damage initiation and final failure for all specimens are extracted from all curves and the average values are given in Fig. 2. It is revealed that final failure load increases with increasing stitch density, as stitches are effective in suppressing delamination growth and eventually raising ultimate strength [1]. However, results also showed that damage initiation load decreases with increasing stitch density. This means that stitched composites are more susceptible to damage initiation at lower loads and this is attributed to the presence of weak resin-rich region around stitch loops, acting as crack initiation sites [2]. Detailed discussion will be made in later sections.

It is further observed that during the *damage propagation* stage (after damage initiation and before final damage failure), densely stitched composite exhibits very smooth curve line, indicating that composite damage is gradual and delamination spread is smooth. However, in moderately stitched and unstitched composites, the curves exhibit some irregular curve pattern with small abrupt load drop, especially at higher displacement, implying sudden damage growth and

delamination propagation. This is due to the fact that when stitches are closely spaced, stitches act as effective crack arrestors for delamination damage, thus preventing sudden delamination widespread.

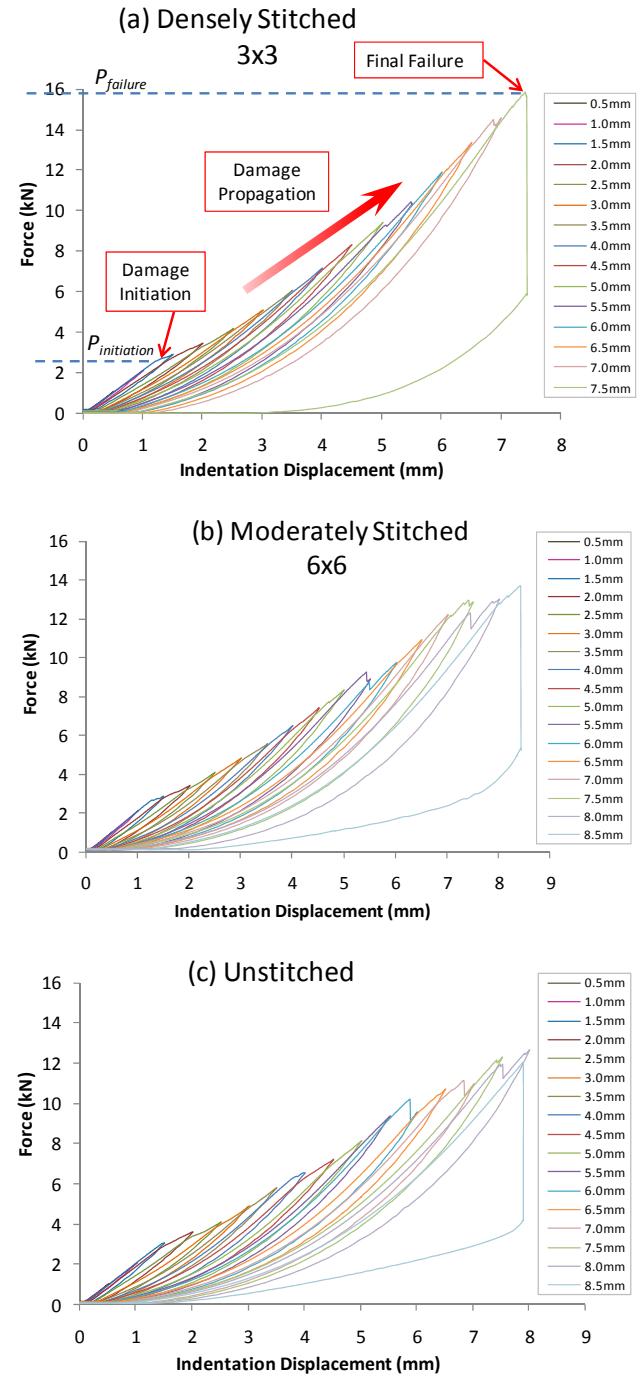


Fig.1. Load-Displacement Curves of (a) Densely Stitched; (b) Moderately Stitched; (c) Unstitched Composites.

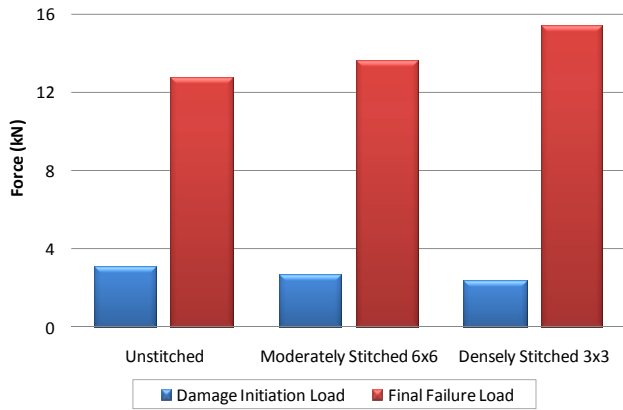


Fig.2. Damage Initiation and Final Failure Force Values for Unstitched and Stitched Composites.

### 3.2 Ultrasonic C-scan Analysis

Typical ultrasonic c-scan images are shown in Fig. 3. These images illustrate the evolution of damage in unstitched and stitched specimens with increasing indentation depth. The red and yellow regions at the center of the images represented the delamination damage area, while the blue region represented the undamaged area. It is obvious that delamination size increases with increasing indentation depth. At  $d=1.5\text{mm}$ , when damage first occurs, it is observed that unstitched specimen has much smaller damage than stitched composites. This is in line with earlier observation that stitched composites are more susceptible to impact damage initiation with lower damage initiation load. Next section will further clarify this with damage mechanisms elucidated by x-ray radiography and micro-computed tomography.

From Fig. 3, we can recognize that the delamination growth in unstitched specimen is fast, reaching support frame boundary at  $d=5.0\text{mm}$  and specimen edge at  $d=6.0\text{mm}$ . The delamination growth of moderately stitched composite is equally fast, but to a smaller extent. In this case, the delamination shape is oblong, similarly observed in low-velocity impact tests [1]. This is attributed to the bending effect of thin laminate. For densely stitched composite, delamination growth is slow and well contained by the stitches. Damage does not reach specimen edge, but extent to support frame boundary at  $d=7.0\text{mm}$ .

The curves of delamination area against indentation depths for all specimens are plotted in Fig. 4.

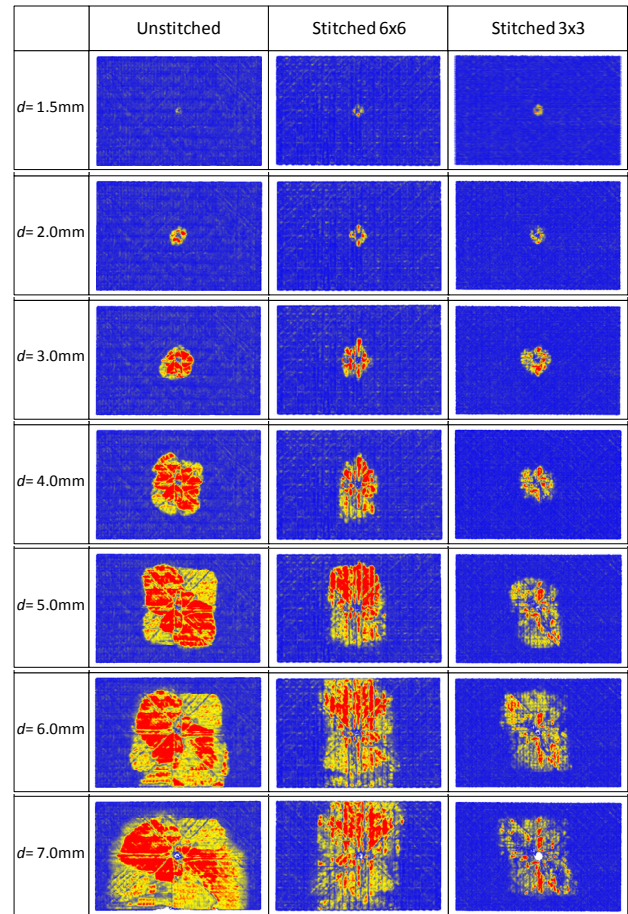


Fig.3. C-scan Images showing Delamination Propagation.

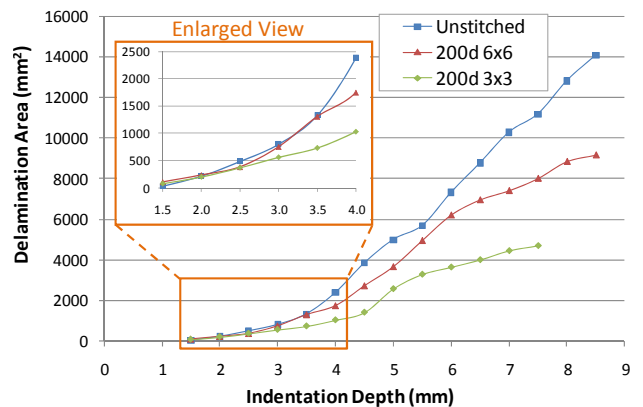


Fig.4. Delamination Area against Indentation Depth.

It is clear that densely stitched configuration can suppress delamination growth effectively as indentation depth increases. Unstitched composite generally has the largest delamination area. Between  $1.5\text{mm} < d < 3.0\text{mm}$ , all curves seem to merge, indicating no effect of stitching when indentation

depth is small. The enlarged view in Fig. 4, however, shows that the effectiveness of stitching actually starts immediately after  $d=2.0\text{mm}$ , and gradually the effect of stitching becomes more prominent when indentation depth is large ( $d>4.0\text{mm}$ ). In fact, at  $d=1.5\text{mm}$ , the delamination of stitched composites are slightly larger than unstitched specimen. Next section covers damage initiation in greater details.

### 3.3 Damage Initiation

As discussed earlier, *damage initiation* is defined as the first observable slope change between 1.0mm to 1.5mm indentation displacement. At  $d=1.5\text{mm}$  of this test, damage closest to initial damage is first observed. It is revealed that stitched composites are more susceptible to damage initiation at lower loads (Fig. 2). This is due to the presence of weak resin-rich region around stitch loops, acting as crack initiation sites, as evidently demonstrated in enlarged x-radiographs shown in Fig. 5. It is observed that multiple stitch-induced matrix cracks are present in densely stitched specimen, and these crack lines are connected by adjacent stitch loops in the in-plane fibre direction. Lesser matrix crack lines are seen in moderately stitched composite, but it is noticed that the delamination damage of both densely and moderately stitched specimens are much larger than unstitched specimen at  $d=1.5\text{mm}$ . Micro-computed tomography images (Fig. 6) show the sectional view of the specimens, further illustrating the extent of initial damage in stitched composites compared to unstitched composites at  $d=1.5\text{mm}$ .

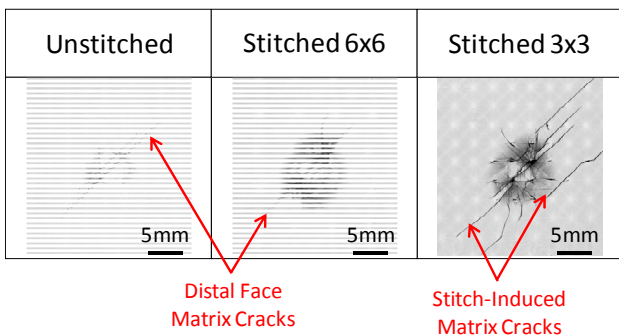


Fig.5. Enlarged X-radiographs at  $d=1.5\text{mm}$ .

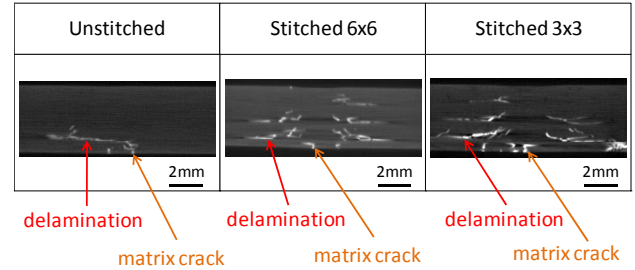


Fig.6. Micro-Computed Tomography Images at  $d=1.5\text{mm}$ .

### 3.4 Damage Propagation

*Damage propagation* is characterized by the extent of delamination growth. As seen in Fig. 3 and 4, it is evident that stitching suppresses delamination propagation, being remarkably effective in densely stitched composite. X-radiographs of test specimens at indentation of  $d=4.5\text{mm}$  (Fig. 7) illustrate that delamination spread is effectively restricted by stitching. The stitching creates closing tractions acting across the crack, which shield the crack tip from the full effect of the crack opening stress. The driving force for propagation of delamination crack is greatly reduced and delamination growth is intensely suppressed. Moreover, delamination crack is effectively arrested by stitches in densely stitched specimens due to the presence of stitches in closer proximity. In authors' earlier work [8], it was revealed that crack arresting and crack bridging account for the main impact resistance mechanisms in stitched composites.

It is worth noting that the interpretation of Fig. 4 should be treated with care, especially when indentation depth is large. This is because boundary saturation occurs when delamination reaches the boundary edge, as seen in Fig. 3, and the effect of boundary influence is not clearly reflected in the measured delamination area.

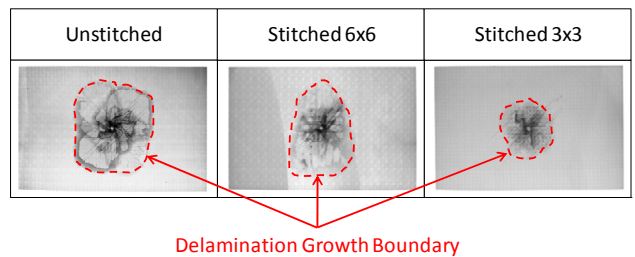


Fig.7. X-radiographs of Specimens at  $d=4.5\text{mm}$ .

### 3.5 Final Failure

*Final failure* is distinguished by a sharp load drop in the load-displacement curve (Fig. 1). From Fig. 2, it is noted that the final failure load for densely stitched is the highest among all specimens. This is rather expected as stitches are successful in resisting delamination damage and would eventually require higher amount of energy for final rupture [9]. However, it is interesting to note that although densely stitched composite failed at higher maximum load, the failure displacement is actually smaller ( $d=7.5\text{mm}$ ), compared to the failure displacement of  $d=8.5\text{mm}$  for moderately stitched and unstitched specimens. This means that the total energy absorption for final failure could be the same for all the specimens, though further investigation needs to be pursued. In authors' earlier work [1], it is revealed that although the energy absorption is the same for differently stitched specimens under low-velocity impact loading, the proportion of energy consumption for damage mechanisms like delamination, matrix cracks and stitch debonding are quantitatively different for different stitch parameters. It is concluded that densely stitched composites consumed more energy for matrix cracks, while moderately stitched composites absorbed higher energy for delamination propagation. Similarly, in this work, the understanding of final failure mechanisms is crucial and important.

Fig. 8 shows the x-radiographs of the specimens at final failure. It is observed that the final failure mode in unstitched and moderately stitched composite is mainly delamination failure, resulting from extensive delamination propagation extending to the edge of the specimens. However, densely stitched composite failed by a different mode, which is primarily penetration consisting of in-plane fibre fracture and matrix crushing. Physical post-mortem examinations of specimens at final failure clearly illustrate the different failure mechanisms (Fig. 9-11). Fig. 9 shows the top and bottom surfaces of densely stitched composite. It is observed that extensive delamination propagation is not present in the final failure mode of densely stitched composite due high interlaminar strength within the ply interface layers. Delamination propagation stops at approximately the boundary of the support frame. Final failure is thus characterized by penetration with matrix crushing and in-plane fibre fracture.

From the bottom surface (Fig. 9b), numerous stitch thread rupture could be clearly observed. Stitch fibre rupture has been found to consume large amount of energy [9].

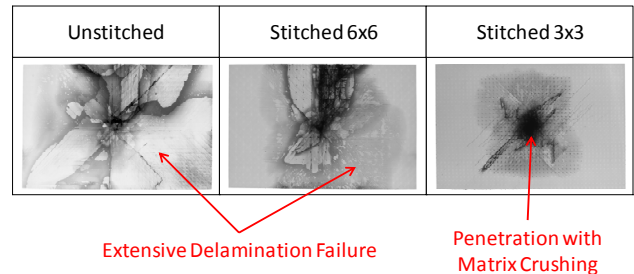


Fig. 8. X-radiographs of Specimens at Final Failure.

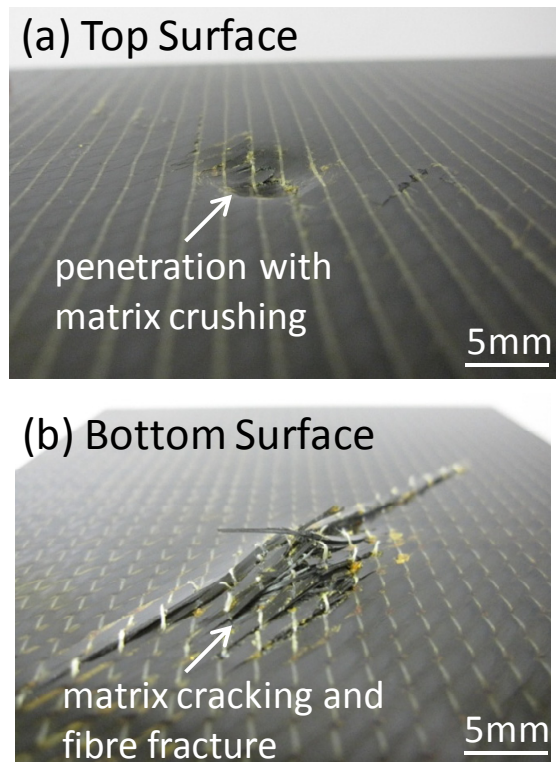


Fig. 9. Post-Mortem Examination of Densely Stitched Composite at Final Failure (a) Top Surface; (b) Bottom Surface.

Fig. 10 and 11 evidently illustrate the extensive delamination damage resulting in final failure of unstitched and moderately stitched specimens. The presence of delamination significantly weakens the composite structure. It is observed that there is less observable matrix crushing and fibre fracture at the indentation location.

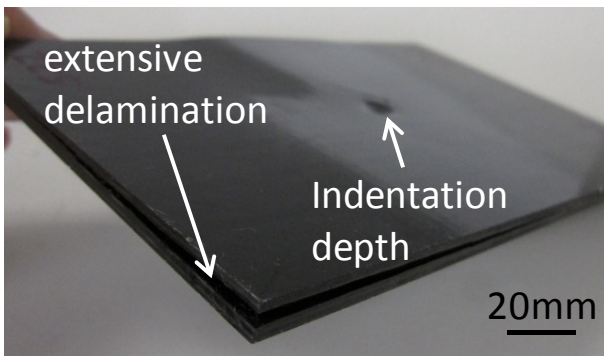


Fig.10. Top Face of Unstitched Composite at Final Failure.

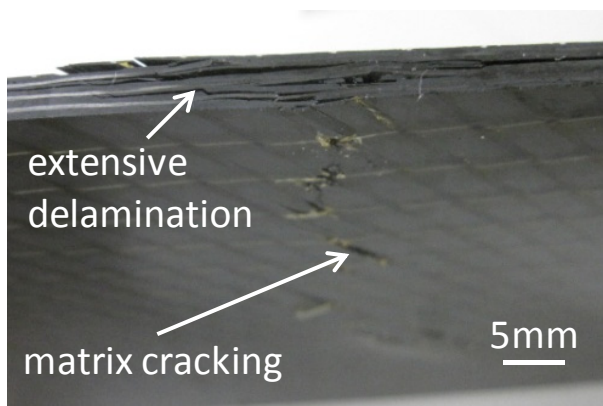


Fig.11. Bottom Face of Moderately Stitched Composite at Final Failure.

#### 4 Conclusions

In this study, progressive damage in stitched composites is studied using quasi-static indentation (QSI) test. Damage progression could be categorized into three stages: *damage initiation*, *damage propagation* and *final failure*.

*Damage initiation* is observable by the first slope change between 1.0mm to 1.5mm displacement. It is revealed that stitched composites are more susceptible to damage initiation at lower loads. This is due to the presence of weak resin-rich region around stitch loops, acting as crack initiation sites.

*Damage propagation* is characterized by the extent of delamination growth. It is evident that stitching suppresses delamination propagation, being remarkably effective in densely stitched composite.

*Final failure* is distinguished by a sharp load drop in the load-displacement curve. It is observed that the final failure mode in unstitched and moderately stitched composite is mainly delamination failure, extending to the edge of the specimens. However,

densely stitched composite failed by a different mode, which is primarily penetration consisting of in-plane fibre fracture and matrix crushing.

#### Acknowledgement

The authors would like to thank Tokyo Metropolitan Government for its financial support from Asian Human Resources Fund under Project Asian Network for Major Cities 21.

#### References

- [1] K.T. Tan, N. Watanabe and Y. Iwahori "Effect of stitch density and stitch thread thickness on low-velocity impact damage of stitched composites". *Compos Part A*, Vol. 41, pp 1857-1868, 2010.
- [2] K.T. Tan, N. Watanabe and Y. Iwahori "Impact damage resistance, response and mechanisms of laminated composites reinforced by through-thickness stitching". *Int J Damage Mech*, in press, doi: 10.1177/1056789510397070.
- [3] K.A. Dransfield, L.K. Jain and Y.W. Mai "On the effects of stitching in CFRPs – I. mode I delamination toughness". *Compos Sci Technol*, Vol. 58, pp 815-827, 1998.
- [4] K.T. Tan, N. Watanabe, Y. Iwahori, H. Hoshi and M. Sano "Interlaminar fracture toughness of vectran-stitched composites - experimental and computational analysis". *J Compos Mater*, Vol. 44, pp 3203-3229, 2010.
- [5] T.E. Tay, G. Liu, V.B.C Tan, X.S. Sun and D.C. Pham "Progressive failure analysis of composites". *J Compos Mater*, Vol. 42, pp 1921-1966, 2008.
- [6] Y. Aoki, H. Suemasu and T. Ishikawa "Damage propagation in CFRP laminates subjected to low velocity impact and static indentation". *Adv Compos Mater*, Vol. 16, pp 45-61, 2007.
- [7] K.T. Tan, N. Watanabe and Y. Iwahori "Stitch fibre comparison for improvement of interlaminar fracture toughness in stitched composites". *J Reinf Plast Compos*, Vol. 30, pp 99-109, 2011.
- [8] K.T. Tan, N. Watanabe and Y. Iwahori "X-ray radiography and micro computed tomography examination of damage characteristics in stitched composites subjected to impact loading". *Compos Part B*, Vol. 42, pp 874-884, 2011.
- [9] K.T. Tan, N. Watanabe and Y. Iwahori "Experimental investigation of bridging law for single fibre using interlaminar tension test". *Compos Struct*, Vol. 92, pp 1399-1409, 2010.